

Coulomb Explosion in Nanosecond Laser Fields

Jie Zhang, Yuzhong Yao, and Wei Kong*



Cite This: *J. Phys. Chem. Lett.* 2020, 11, 1100–1105



Read Online

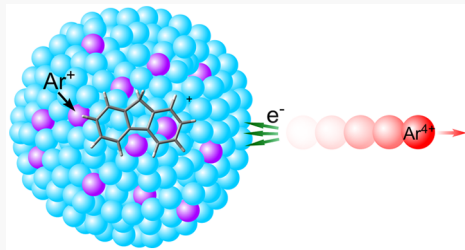
ACCESS |

Metrics & More

Article Recommendations

Supporting Information

ABSTRACT: We report experimental observations of Coulomb explosion using a nanosecond laser at 532 nm with intensities less than 10^{12} W/cm^2 . We observe multiply charged atomic ions Ar^{n+} ($1 \leq n \leq 7$) and C^{n+} ($1 \leq n \leq 4$) from argon clusters doped with molecules containing aromatic chromophores. The yield of Ar^{n+} depends on the size of the cluster, the number density, and the photostability of the dopant. We propose that resonant absorption of Ar_N^{n+} achieves a high degree of ionization, and the highly positively charged cluster has the capability to strip electrons from the evaporating Ar^+ on the surface of the cluster prior to Coulomb explosion, forming Ar^{n+} .



Laser–matter interactions have long been categorized into “strong” and “weak” field regimes.¹ As a unique phenomenon of strong fields, Coulomb explosion (CE) and its characteristic multiply charged atomic ions (MCAI) have been considered a result of field ionization achievable using ultrafast lasers, on the order of 10^{15} W/cm^2 .^{2,3} Although nanosecond lasers can achieve intensities of 10^{12} W/cm^2 , these intensities are far below the threshold for field ionization of most atoms, with the exception of alkali metals.¹ Hence, CE and MCAI are considered rare if possible at all in nanosecond laser fields. However, counter evidence to the general belief has been reported first in 1981 by the Wittig group^{4,5} and more recently by the Li group and the Vatsa group.^{6–14} The presence of MCAI from nanosecond laser fields deserves a systematic investigation.

On the basis of the reports of the Li group and the Vatsa group,^{6–14} production of MCAI requires clusters, either pure molecular clusters or rare gas clusters doped with neutral molecules, at excitation wavelengths ranging from the infrared (1064 nm) to the visible, while UV excitation is ineffective. Power dependence of the yield of MCAI, including all atom types present in the cluster except for hydrogen, reveals a nonlinear process, but the exponent of the dependence is mostly below 3, far smaller than the number of photons required to produce a MCAI.¹⁵ Armstrong et al. attributed the production of U^{2+} and W^{2+} from UF_6 and WF_6 to “giant resonances” of the heavy atoms due to their high density of states.¹⁶ However, the molecular species from the Li group and the Vatsa group contain no heavy atoms. Wang et al. then proposed that the trapped electrons from nonresonant multiphoton ionization (MPI) can be accelerated in the laser field via inverse bremsstrahlung (IB), and the resulting energetic electrons can produce MCAI through electron impact ionization.¹⁷ To explain the discrepancy of the relatively low kinetic energies of the observed electrons (less than 25 eV¹⁸) and the comparatively much higher ionization

energies of some outer-shell electrons (>25 eV for all triply charged nontransition metal atoms),¹⁵ screening effects of the trapped nonlocalized electrons are invoked.

Two major issues face the model by Wang et al.¹⁷ Classically, when a free electron is pushed against a nucleus by an oscillating electric field, the electron can retain some of the energy from the field. The rate of energy gain is proportional to the ponderomotive energy and the rate of collisions between the electron and nearby nuclei. Quantum mechanically, an electron can only absorb one whole photon at a time, and the classical model of IB heating is therefore only valid when the ponderomotive energy far exceeds the photon energy.¹⁹ At 532 nm in a field of 10^{11} W/cm^2 , the ponderomotive energy is 3 meV,^{2,3} while the energy of one photon is 2.3 eV. Hence, in this regime, the classical theory does not apply.²⁰ Another issue is the observed charge distribution of the MCAI.¹⁷ If MCAI are produced through sequential electron impact ionization, lower charge states should be preferentially populated compared to higher charge states, unless available neutral atoms have been exhausted.^{6–14} Experimentally, the opposite has been routinely observed.^{6–14}

In an attempt to resolve these issues, we performed experiments similar to those of the Li and Vatsa groups,^{6–14} but we used compounds with much lower vapor pressures as cluster dopants, including indole ($\text{C}_8\text{H}_7\text{N}$), fluorene ($\text{C}_{13}\text{H}_{10}$), 2-iodofluorene (IFl, $\text{C}_{13}\text{H}_9\text{I}$), 2-bromofluorene (BrFl, $\text{C}_{13}\text{H}_9\text{Br}$), and pyrene ($\text{C}_{16}\text{H}_{10}$). Variations of the heating temperature and the stagnation pressure of argon allowed systematic variations of the composition and size of the doped clusters. We observed Ar^{n+} and C^{n+} ($n \geq 1$), in general

Received: January 9, 2020

Accepted: January 24, 2020

Published: January 24, 2020

agreement with previous reports.^{6–14} However, as the vapor pressure of the dopant increased, the yield of MCAI changed nonmonotonically. In addition, we also observed that the rise of Ar^{n+} superseded that of the sample MCAI in some cases. On the basis of these results, we tentatively propose a modified mechanism of energy accumulation and MCAI formation. We believe that the primary mode of energy absorption is resonant multiphoton absorption, in-line with the idea of “giant resonances”.¹⁶ The solid argon cluster can accumulate a large number of charges during a very short time (<1 ps), creating a strong Coulomb potential on the surface of the cluster. Thermal evaporation of any surface atom or ion would result in the electrons of the departing species being stripped back to the cluster in this Coulomb potential, ionizing the departing species and producing MCAI. Although qualitative, this evaporation model agrees with most reported observations, both from this work and from prior reports.^{6–14}

The experimental setup is a standard differentially pumped pulsed supersonic molecular beam apparatus, with mutual orthogonality among the molecular beam, the laser beam, and a time-of-flight (TOF) mass spectrometer. The solid sample is directly enclosed in the heated pulse valve (nozzle diameter: 0.5 mm) and mixed with the argon carrier gas. At a vapor pressure of 10 Pa and a stagnation pressure 10^6 Pa (10 atm), on average a cluster containing 1000 Ar should have at most one neutral dopant. The excitation laser is the second harmonic of a Q-switched Nd:YAG laser (Quantel Brilliant) at 532 nm with a duration of 10 ns, pseudo Gaussian in both spatial and time profile, focused using a lens of 25 cm in focal length, with a resulting power density between 10^{10} and 10^{12} W/cm².

We have characterized the size distributions of the doped clusters using the fourth harmonic of the same Nd:YAG at 266 nm at a power density of 7×10^5 W/cm². Between stagnation pressures of 4 and 17 atm, the most probable cluster size increases from 150 to 1500 argon atoms. The TOF mass spectra of BrF₁ are shown in Figure S1, and the resulting sizes and size distributions are shown in Figure S2 and listed in Table SI (Supporting Information). These sizes are consistent within 20% for all the compounds investigated in this work. Although different in the size and shape of the nozzle, these numbers are also in general agreement with those from Hagena and Obert.²¹ We consider these values the lower limits because of the decreasing sensitivity of the microchannel plate detector with increasing ion masses and potential fragmentation of the cluster upon ionization.

Increasing the power density at 266 nm to 10^{10} W/cm² via a focal lens only resulted in molecular fragments of the dopant, without any detectable signal of MCAI. However, after removing the frequency doubling unit and reducing the power of the laser at 532 nm to the same level of 10^{10} W/cm², we can observe abundant MCAI. Figure 1 shows the TOF mass spectra obtained from fluorene doped clusters of two different sizes. While the intensities of singly charged atomic ions are relatively consistent, the intensities of Ar^{n+} are sensitive to the cluster size, with the yields of Ar^{n+} being consistently higher for larger clusters. Furthermore, the charge distribution of Ar^{n+} is nonstatistical, with Ar^{3+} the most abundant. The widths of the singly and multiply charged ions are also noticeably different, with broader peaks indicative of higher kinetic energies for higher charge-state ions.

Figure 2 shows the dependence of Ar^{n+} from BrF₁ on the cluster size. With increasing cluster sizes, the yields of lower

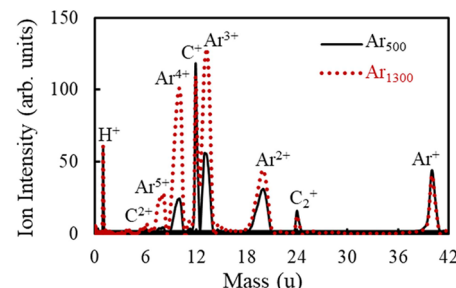


Figure 1. Mass spectra of fluorene in laser fields of 10^{11} W/cm² at 532 nm. The two traces were obtained at two different estimated cluster sizes as labeled.

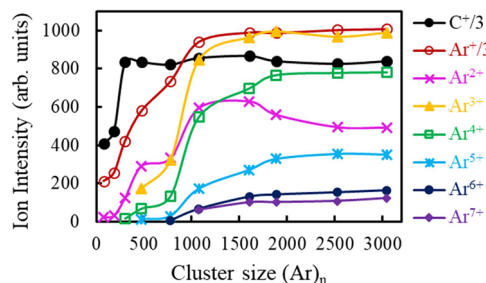


Figure 2. Size dependence of Ar^{n+} and C^+ from BrF₁ doped argon clusters. The cluster sizes are the most probable size at the corresponding stagnation pressures.

charge-state MCAI first increase and then reach a plateau or even start to decrease, while the yields of higher charge-state MCAI only start to increase at larger cluster sizes. We note here that, different from the case of fluorene, the intensities of singly charged C^+ and Ar^+ are the most intense in BrF₁.

The dependence of the yield of MCAI on the vapor pressure of the sample is more complicated, as seen in Figure 3a. Although the increase of C^+ is expected, the increase of Ar^{n+} with vapor pressure is not immediately intuitive. In fact, we might expect competitive behavior between the atomic species Ar^{n+} and C^{n+} . More puzzling is the abundance of Ar^{4+} : it peaks at 20 Pa, decreases sharply until 30 Pa, and then slowly declines. The subtle oscillatory behavior at higher vapor pressures is likely due to variations in the behavior of the valve.

This preference for highly charged MCAI at low vapor pressures is a consistent pattern among all the compounds that we have studied, including indole, fluorene, IFl, BrF₁, and pyrene. Data from BrF₁ are similar to those from IFl, in both charge-state distributions and overall ion intensity. Figure 3b shows the abundance of the MCAI from fluorene. The overall intensity of the MCAI is much higher, although no quantitative comparison should be made because of minor differences in the experimental conditions. Even clearer in Figure 3b is the relative rate of increase of Ar^{4+} to that of C^+ : Ar^{4+} increases much faster below 150 Pa.

Our results are in general agreement with those in the literature,^{6–14} but several new observations are only possible under the low vapor pressure conditions. We have also recorded the power dependence of the ion yields, and the fitting result is provided as Supporting Information: the exponent of the laser power is 1.5 for Ar^{5+} and 1.25 for C^+ . These values are only slightly lower than those in the literature.^{6–14} We note that to remove one electron from Ar^{4+} to Ar^{5+} , 33 photons at 532 nm are needed.¹⁵ The power

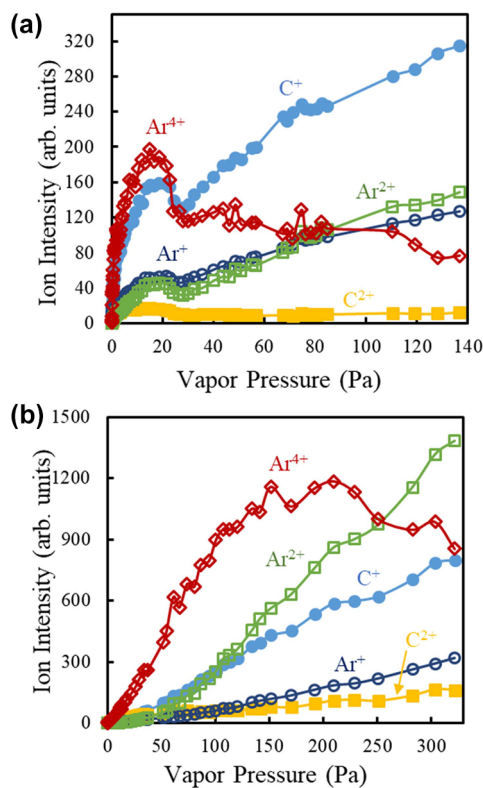


Figure 3. Abundance of argon and carbon ions from Ar_{1300} doped with iodofluorene (a) and fluorene (b) at different vapor pressures of the dopants.

dependence in these measurements is not representative of the number of photons involved in the process. The fact that Ar^{4+} can be more intense than Ar^{2+} and Ar^+ while all absolute abundances are increasing with increasing laser intensity contradicts the model of sequential electron impact ionization. In addition, BrF_3 and IF_3 are more dissociative than fluorene upon photoexcitation, and the yield of MCAI from these halogenated compounds is much lower.

We propose a modified model of Wang et al.¹⁷ to account for the observed patterns of MCAI. The energy levels of the relevant species are shown in Figure 4. Direct ionization (or

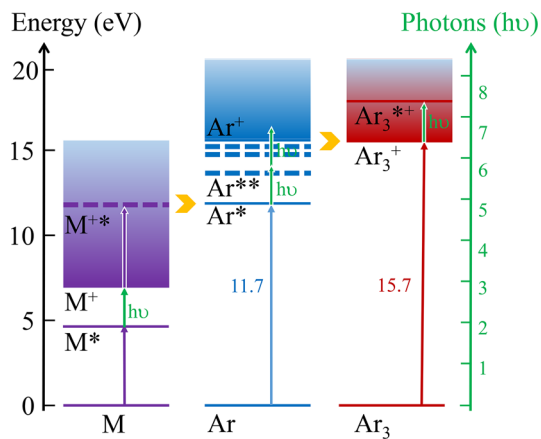


Figure 4. Relevant energy levels of the molecular species (M), argon atom (Ar), and argon trimer (Ar_3) in the proposed mechanism of Coulomb explosion. The scale is relative, with the ground state of all species lined up for direct comparisons of excitation energies.

excitation) of argon at 532 nm requires 7 (or 5) photons, which is impossible under our field conditions, as evidenced by our failed attempt to ionize pure argon clusters. However, direct ionization of the molecular species only requires 3 photons. More importantly, all the molecular species in this study contain the aromatic chromophore, and both the neutral and cationic chromophore^{22–25} have a resonance near 266 nm, achievable via two photons at 532 nm. Hence, a 5-photon excitation of the dopant via two resonant states can reach the first excited state of argon, and resonant energy transfer to the surrounding argon atoms accomplishes the first step of Ar excitation at 11.7 eV.²⁶ Further absorption by the excited-state argon atom (resonant via the $3p^53d^1$ manifold) should then be enough to achieve ionization.¹⁵

Once the first Ar^+ is formed, the charge can be localized as Ar_2^+ or Ar_3^+ , and due to resonant absorption of Ar_3^+ , the number of Ar_3^+ would rise exponentially. The absorption cross sections of Ar_N^+ ($N \geq 3$) at 532 nm are on the order of 10^{-16} cm^2 ,^{27,28} comparable to those of the collective excitations in Ag_N ions^{29,30} and in nanoplasmas produced in strong fields.² This means that, for each Ar_3^+ , there are 7 photons available for absorption in 26 fs at a power density of 10^{12} W/cm^2 , producing one new Ar^+ , thereby a new Ar_3^+ , and doubling the number of Ar_3^+ . Only 10 cycles of doubling (on the order of 260 fs) are needed to produce 1000 Ar_3^+ . This process, to some degree, can also be considered as “ionization ignition”.³¹ The mean-free-path of low energy electrons (<1 eV) in argon is longer than 4 nm,³² while the radius of Ar_{1000} is only 2 nm; hence, a highly positively charged argon cluster, quite different from a quasi-neutral nanoplasma, can be formed. We note here that, for krypton and xenon clusters,⁸ which were also observed to produce MCAI in this regime, the corresponding transition shifts to lower energies, but the width of the transition is broad, and sufficient oscillator strength still remains at 532 nm, particularly when the polydispersity of the cluster size is included. Hence, this specific resonance of Ar_3^+ (or Ar_N^+) is not crucial to the general mechanism. For doped helium clusters, however, because of the high excitation energy at 22 eV, no MCAI should be observed. This was indeed confirmed empirically.

The highly charged cluster is unstable and will explode under Coulomb repulsion. The binding energy of an Ar_N^+ cluster with $N > 20$ is 50 meV per neutral atom;^{33,34} hence, the total binding energy from a solvation shell of 30 neutral atoms (at 1.5 eV³⁵) is comparable to the repulsive Coulomb potential energy between two Ar^+ separated by 1 nm, assuming a dielectric constant of vacuum.³⁶ Therefore, at a density of $2.4 \times 10^{22} \text{ atoms/cm}^3$ for solid argon,³⁷ the cluster becomes unstable when the ionization level exceeds 3%. However, if the rate of ionization is faster than the rate of hole transfer, a hot ionic core surrounding the dopant can be formed, while other regions away from the dopant remain bound via the van der Waal's potential. The rate of hole transfer in solid argon is $0.01 \text{ cm}^2/\text{V s}$,³⁸ hence, it takes 1.6 ps for an Ar^+ to move from 1 to 2 nm away from a unit charge. The higher the charge, the shorter the transfer time. Additionally, the time scale of Coulomb explosion can be estimated by calculating the time it takes to displace two Ar^+ without the solvation shell from 1 to 2 nm, and the result is slightly more than 0.6 ps. These time scales for charge transfer and Coulomb explosion are long enough for the outer-shell electrons from an evaporating atom or ion to escape the field of the nucleus and to return to the field of the highly charged cluster.

With a high degree of ionization, thermal evaporation of surface Ar or Ar^+ results in electron-stripping from the departing species. The radius of a cluster is determined by the number of atoms N and density ρ , and for a fixed degree of ionization Y , the Coulomb potential from the cluster at the surface of the cluster is (in Atomic Units u):

$$|V_{\text{cluster}}| = \frac{N \cdot Y}{\left(\frac{N \cdot 3}{\rho \cdot 4\pi}\right)^{1/3}} = N^{2/3} Y \left(\frac{4\pi}{3}\rho\right)^{1/3} \quad (1)$$

When this potential is comparable to that from the nucleus for a 3p electron, the departing atom or ion could lose the electron to the remaining cluster. The effective charge experienced by a 3p electron ranges from 1 (most shielded scenario) to 6 u (least shielded), and assuming a radius of 1.3 u for the atomic orbital,³⁹ the atomic potential ranges between 0.75 and 4.5 u. Figure 5 shows the highest charge state

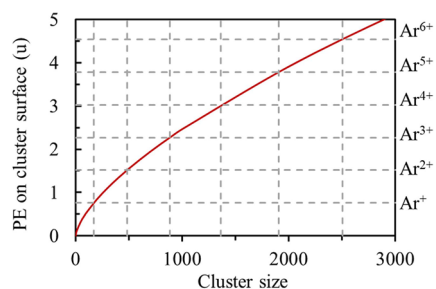


Figure 5. Qualitative Coulomb potential energies on the surface of argon clusters of different sizes, assuming that 10% of the argon atoms are ionized throughout the cluster. When this energy is comparable to the Coulomb potential energy from the nucleus of an Ar^{n+} (calculated assuming an orbital radius of 1.3 u and an effective charge of n u), as illustrated by the horizontal lines and labeled on the right axis, an electron can be stripped from the departing species, resulting in formation of Ar^{n+} .

energetically achievable for each cluster size assuming a 10% ionization level. For example, if a neutral argon atom is to leave a cluster of 140 atoms with 14 Ar^+ , it could be ionized to form Ar^+ . From Figure 5, to produce Ar^{5+} , the cluster has to contain 190 Ar^+ with a size of 1900. Hence, there is a cutoff size for each MCAI at a fixed degree of ionization, and a larger cluster produces a more highly charged MCAI. We note that when the effect of tunneling is included, production of MCAI becomes possible even if the cluster is slightly smaller than the cutoff size.

We caution here that this model is only qualitative, ignoring the change of the effective radius of the 3p electron at different levels of ionization. Even at this very high degree of ionization, the necessary cluster size to observe each MCAI still exceeds the size observed from the experiment. We attribute this discrepancy partly to the inadequate measurement of the cluster sizes, as explained earlier. In addition, the cluster beam has a wide size distribution, and the size range also increases with increasing stagnation pressure (see Supporting Information). The long tail of the size distribution at larger sizes could easily contribute to the observed MCAI even when the most probable size is still below the threshold.

This evaporation model is different from typical strong field CE achieved via ultrafast lasers,⁴⁰ but it is similar to that proposed by Wabnitz et al. on ionization of Xe_n using a free-electron laser.⁴¹ In essence, the MCAI observed in this

experiment are not directly ionized; rather, they are formed as they leave the cluster. The massive amount of photon energy required to generate a single MCAI is supplied by energy accumulation through resonant absorption by molecular ions and rare gas cluster ions. The argon cluster ions are an analogue of the “giant resonance” in heavy atoms.¹⁶ The ability of the cluster to accommodate a large number of charges is crucial to the formation of MCAI; the cluster is far from a quasi-neutral nanoplasma.

This model suggests that the more stable the molecular species, the higher the yield of the MCAI. Hence, the intensity of the MCAI from fluorene should be higher than that from the more dissociative halogenated fluorenes, as observed experimentally. In fact, we have also performed the same measurements using I_2 as dopant, and within the range of experimental parameters reported in this work, both I^{n+} and Ar^{n+} ($n > 1$) were barely detectable. We attribute this failure to the facile dissociation of iodine upon photoabsorption at 532 nm. The kinetic energy release during bond fission either reduces the size of the cluster or induces cluster fission into smaller clusters,^{42,43} and both scenarios are detrimental to the formation of MCAI.

The same mechanism can be used to explain the wavelength dependence of the CE process. A higher energy photon tends to impart more extra energy to the molecular species, opening more channels of dissociation.

The effect of the sample vapor pressure on the abundance of MCAI can also be explained by this model. The function of the molecular species is limited to initiation of the chain absorption process; hence, more than one molecule in the cluster is not beneficial to the formation of MCAI. On the contrary, more covalent bonds from more doped molecules increase the chance of large energy release upon photoabsorption and dissociation, resulting in cluster fission or size reduction.^{42,43} Consequently, at higher vapor pressures, the abundance of higher charge-state MCAI decreases. However, in pure molecular clusters studied by the Li group and the Vatsa group,^{6–14} each molecule serves as both an initiation and absorption center, beneficial to the formation of a highly charged cluster for electron stripping.

The location of the dopant in the cluster is unknown, although given the high polarizability of the dopants and the overwhelming number of argon atoms, there is good reason to believe that the dopant molecule is preferentially inside the cluster. The faster rise of Ar^{n+} with vapor pressure than that of C^{n+} in the low vapor pressure regions of Figure 3 is in general agreement with this consideration. Evaporation prefers the surface Ar atoms over the interior dopant C atoms. Nevertheless, we did observe small amounts of singly charged molecular fragments (C_2^+) and multiply charged carbon atoms, and they could be due to surface-bound dopants or from minor channels related to dissociation of molecules located near the surface of the cluster.

This evaporation model is consistent with increased velocities of higher charge-state ions, and it also implies that the MCAI should be spatially isotropic upon formation, because the evaporation process bears no relation to the excitation step of the dopant. In the report of Wang et al., no anisotropy in the ion yields was observed.⁴⁴

We present CE in nanosecond laser fields from rare gas clusters doped with semivolatile molecular species. The excitation pathway involves near-resonant excitation of the molecular species, energy transfer to the surrounding argon

atoms, and ionization of Ar. The ionized argon clusters further resonantly absorb a massive amount of photon energy for local ionization, forming a highly charged ionic core. Evaporation of Ar or Ar⁺ from the cluster surface results in electron stripping from the departing species. This model explains the non-statistical abundance of Arⁿ⁺, and is consistent with almost all experimental observations.

■ ASSOCIATED CONTENT

SI Supporting Information

The Supporting Information is available free of charge at <https://pubs.acs.org/doi/10.1021/acs.jpcllett.0c00092>.

Discussion of measurements of cluster sizes, mass spectra, list of Ar_n sizes, power dependence graph, discussion of elimination of possible artifact of the experiment. ([PDF](#))

■ AUTHOR INFORMATION

Corresponding Author

Wei Kong — Department of Chemistry, Oregon State University, Corvallis, Oregon 97331, United States; orcid.org/0000-0003-3882-5019; Phone: 541-737-6714; Email: wei.kong@oregonstate.edu; Fax: 541-737-2062

Authors

Jie Zhang — Department of Chemistry, Oregon State University, Corvallis, Oregon 97331, United States

Yuzhong Yao — Department of Chemistry, Oregon State University, Corvallis, Oregon 97331, United States

Complete contact information is available at:

<https://pubs.acs.org/10.1021/acs.jpcllett.0c00092>

Notes

The authors declare no competing financial interest.

■ ACKNOWLEDGMENTS

This material is based upon work supported by National Institute of General Medical Sciences (1R01GM101392-01A1) from the National Institutes of Health and by the National Science Foundation under Grant No. 1838522. We are particularly grateful to the suggestion of Dr. John Loeser on the possibility of electron stripping by a highly charged cluster. Discussions with Dr. Darrah T. Thomas are also deeply appreciated. We are also appreciative of the contribution of Andrew Oswalt in the early stages of this project.

■ REFERENCES

- (1) Reinhard, P. G.; Suraud, E. *Introduction to Cluster Dynamics*; Wiley-VCH Verlag GmbH & Co. KGaA: Weinheim, 2004.
- (2) Fennel, T.; Meiwes-Broer, K. H.; Tiggensebaumer, J.; Reinhard, P. G.; Dinh, P. M.; Suraud, E. Laser-Driven Nonlinear Cluster Dynamics: From Single- and Multiphoton Excitations to the Strong-Field Domain. *Rev. Mod. Phys.* **2010**, *82*, 1793–1842.
- (3) Saalmann, U.; Siedschlag, C.; Rost, J. M. Mechanisms of Cluster Ionization in Strong Laser Pulses. *J. Phys. B: At., Mol., Opt. Phys.* **2006**, *39*, R39–R77.
- (4) Stuke, M.; Reisler, H.; Wittig, C. Monitoring Uranium Hexafluoride Photodissociation Via Laser Multiphoton Ionization. *Appl. Phys. Lett.* **1981**, *39*, 201–203.
- (5) Stuke, M.; Wittig, C. Multiply Charged Atomic and Molecular Ions from Laser Multiphoton Ionization of Uranium Hexafluoride. *Chem. Phys. Lett.* **1981**, *81*, 168–169.
- (6) Kong, X.; Luo, X.; Niu, D.; Li, H. Cluster Assistant Generation of C²⁺ and C³⁺ Ions in Nanosecond Laser Ionization of Seeded Benzene Beam. *Chem. Phys. Lett.* **2004**, *388*, 139–143.
- (7) Zhao, W.; Wang, W.; Qu, P.; Hou, K.; Li, H. Multiple Ionization of CH₃I Clusters by Nanosecond Laser: Electron Energy Distribution and Formation Mechanism of Multiply Charged Ions. *Chem. Phys. Lett.* **2012**, *543*, 55–60.
- (8) Luo, X.; Li, H.; Niu, D.; Wen, L.; Liang, F.; Wang, B.; Xiao, X. Cluster-Assisted Multiple Ionization of Xenon and Krypton by a Nanosecond Laser. *Phys. Rev. A: At., Mol., Opt. Phys.* **2005**, *72*, 013201.
- (9) Zhang, N.; Wang, W.; Zhao, W.; Han, F.; Li, H. Multiply Ionization of Diethyl Ether Clusters by 532 nm Nanosecond Laser: The Influence of Laser Intensity and the Electron Energy Distribution. *Chem. Phys.* **2010**, *373*, 181–185.
- (10) Niu, D.; Li, H.; Liang, F.; Wen, L.; Luo, X.; Wang, B.; Qu, H. Coulomb Explosion of Ammonia Clusters Induced by Intense Nanosecond Laser at 532 and 1064 nm: Wavelength Dependence of the Multicharged Nitrogen Ions. *J. Chem. Phys.* **2005**, *122*, 151103.
- (11) Niu, D.; Li, H.; Wang, W.; Xiao, X.; Luo, X.; Zhang, N.; Hou, K. Cluster-Assisted Generation of Multiply Charged Ions in Nanosecond Laser Ionization of Seeded Furan Beam at 532 and 1064 nm. *Mol. Phys.* **2008**, *106*, 1389–1395.
- (12) Niu, D.; Li, H.; Liang, F.; Luo, X.; Wen, L. Controllable Generation of Highly Stripped Ions with Different Charges by Nanosecond Laser Ionization of Clusters at Different Wavelengths. *Appl. Phys. Lett.* **2005**, *87*, 034103.
- (13) Badani, P.; Das, S.; Sharma, P.; Vatsa, R. K. Mass Spectrometric and Charge Density Studies of Organometallic Clusters Photoionized by Gigawatt Laser Pulses. *Mass Spectrom. Rev.* **2017**, *36*, 188–212.
- (14) Das, S.; Badani, P. M.; Sharma, P.; Vatsa, R. K. Coulomb Explosion Phenomenon Using Gigawatt Intensity Laser Fields: An Exotic Realm of Laser-Cluster Interaction. *Curr. Sci.* **2011**, *100*, 1008–1019.
- (15) CRC Handbook of Chemistry and Physics; Lide, D. R., Ed.; CRC Press LLC: Boca Raton, 2004.
- (16) Armstrong, D. P.; Harkins, D. A.; Compton, R. N.; Ding, D. Multiphoton Ionization of Uranium Hexafluoride. *J. Chem. Phys.* **1994**, *100*, 28–43.
- (17) Wang, W.; Li, H.; Niu, D.; Wen, L.; Zhang, N. Cluster-Assisted Multiple-Ionization of Methyl Iodide by a Nanosecond Laser: Wavelength Dependence of Multiple-Charge Ions. *Chem. Phys.* **2008**, *352*, 111–116.
- (18) Sharma, P.; Vatsa, R. K.; Kulshreshtha, S. K.; Jha, J.; Mathur, D.; Krishnamurthy, M. Energy Pooling in Multiple Ionization and Coulomb Explosion of Clusters by Nanosecond-Long, Megawatt Laser Pulses. *J. Chem. Phys.* **2006**, *125*, 034304.
- (19) Friedland, L. Correspondence Principle in Multiphoton Inverse Bremsstrahlung. *J. Phys. B: At. Mol. Phys.* **1979**, *12*, 409–418.
- (20) Seely, J. F.; Harris, E. G. Heating of a Plasma by Multiphoton Inverse Bremsstrahlung. *Phys. Rev. A: At., Mol., Opt. Phys.* **1973**, *7*, 1064–1067.
- (21) Hagen, O. F.; Obert, W. Cluster Formation in Expanding Supersonic Jets: Effect of Pressure, Temperature, Nozzle Size, and Test Gas. *J. Chem. Phys.* **1972**, *56*, 1793–1802.
- (22) Vala, M.; Szczepanski, J.; Pauzat, F.; Parisel, O.; Talbi, D.; Ellinger, Y. Electronic and Vibrational Spectra of Matrix-Isolated Pyrene Radical Cations: Theoretical and Experimental Aspects. *J. Phys. Chem.* **1994**, *98*, 9187–9196.
- (23) Malloci, G.; Mulas, G.; Joblin, C. Electronic Absorption Spectra of PAHs up to Vacuum UV: Towards a Detailed Model of Interstellar PAH Photophysics. *Astron. Astrophys.* **2004**, *426*, 105–117.
- (24) Chalyavi, N.; Catani, K. J.; Sanelli, J. A.; Dryza, V.; Bieske, E. J. Gas-Phase Electronic Spectrum of the Indole Radical Cation. *Mol. Phys.* **2015**, *113*, 2086–2094.
- (25) Johnson, P. M. The Jahn-Teller Effect in the Lower Electronic States of Benzene Cation. I. Calculation of Linear Parameters for the e_{2g} Modes. *J. Chem. Phys.* **2002**, *117*, 9991–10000.

(26) Chan, W. F.; Cooper, G.; Guo, X.; Burton, G. R.; Brion, C. E. Absolute Optical Oscillator Strengths for the Electronic Excitation of Atoms at High Resolution. III. The Photoabsorption of Argon, Krypton, and Xenon. *Phys. Rev. A: At., Mol., Opt. Phys.* **1992**, *46*, 149–171.

(27) Haberland; von, I. B.; Kolar; Kornmeier; Ludewigt; Risch. Electronic and Geometric Structure of Ar_n^+ and Xe_n^+ Clusters: The Solvation of Rare-Gas Ions by Their Parent Atoms. *Phys. Rev. Lett.* **1991**, *67*, 3290–3293.

(28) Levinger, N. E.; Ray, D.; Alexander, M. L.; Lineberger, W. C. Photoabsorption and Photofragmentation Studies of Argon (Ar_n^+) Cluster Ions. *J. Chem. Phys.* **1988**, *89*, 5654–5662.

(29) Tiggesbaeumker, J.; Koeller, L.; Meiwas-Broer, K.-H. Bound-Free Collective Electron Excitations in Negatively Charged Silver Clusters. *Chem. Phys. Lett.* **1996**, *260*, 428–432.

(30) Tiggesbaeumker, J.; Koeller, L.; Meiwas-Broer, K. H.; Liebsch, A. Blue Shift of the Mie Plasma Frequency in Silver Clusters and Particles. *Phys. Rev. A: At., Mol., Opt. Phys.* **1993**, *48*, R1749–R1752.

(31) Rose-Petruck, C.; Schafer, K. J.; Wilson, K. R.; Barty, C. P. J. Ultrafast Electron Dynamics and Inner-Shell Ionization in Laser-Driven Clusters. *Phys. Rev. A: At., Mol., Opt. Phys.* **1997**, *55*, 1182–1190.

(32) Buckman, S. J.; Lohmann, B. Low-Energy Total Cross Section Measurements for Electron Scattering from Helium and Argon. *J. Phys. B: At. Mol. Phys.* **1986**, *19*, 2547–2564.

(33) Chen, H. H.; Lim, C. C.; Aziz, R. A. The Enthalpies of Sublimation and Internal Energies of Solid Argon, Krypton, and Xenon Determined from Vapor Pressures. *J. Chem. Thermodyn.* **1978**, *10*, 649–659.

(34) Engelking, P. C. Determination of Cluster Binding Energy from Evaporative Lifetime and Average Kinetic Energy Release: Application to Carbon Dioxide and Argon Ion(1+) ($(\text{CO}_2)_n^+$ and Ar_n^+) Clusters. *J. Chem. Phys.* **1987**, *87*, 936–940.

(35) Ikegami, T.; Kondow, T.; Iwata, S. The Geometric and Electronic Structures of Argon Cluster Ions(1+) (Ar_n^+ ($n = 3–27$))). *J. Chem. Phys.* **1993**, *98*, 3038–3048.

(36) Doniach, S.; Huggins, R. Short-Range Forces and the Dielectric Properties of Solid Argon. *Philos. Mag.* **1965**, *12*, 393–408.

(37) Dobbs, E. R.; Figgins, B. F.; Jones, G. O. Properties of Solid Argon. *Nuovo Cimento* **1958**, *9*, 32–35.

(38) Le Comber, P. G.; Loveland, R. J.; Spear, W. E. Hole Transport in the Rare-Gas Solids Ne, Ar, Kr, and Xe. *Phys. Rev. B* **1975**, *11*, 3124.

(39) Bartell, L. S.; Brockway, L. O. The Investigation of Electron Distribution in Atoms by Electron Diffraction. *Phys. Rev.* **1953**, *90*, 833–838.

(40) Komar, D.; Kazak, L.; Almassarani, M.; Meiwas-Broer, K. H.; Tiggesbäumker, J. Highly Charged Rydberg Ions from the Coulomb Explosion of Clusters. *Phys. Rev. Lett.* **2018**, *120*, 133207.

(41) Wabnitz, H.; Bittner, L.; de Castro, A. R. B.; Doehrmann, R.; Guertler, P.; Laarmann, T.; Laasch, W.; Schulz, J.; Swiderski, A.; von Haeften, K.; Moeller, T.; Faatz, B.; Fateev, A.; Feldhaus, J.; Gerth, C.; Hahn, U.; Saldin, E.; Schneidmiller, E.; Sytchev, K.; Tiedtke, K.; Treusch, R.; Yurkov, M. Multiple Ionization of Atom Clusters by Intense Soft X-Rays from a Free-Electron Laser. *Nature* **2002**, *420*, 482–485.

(42) Harris, C.; Baptiste, J.; Lindgren, E. B.; Besley, E.; Stace, A. J. Coulomb Fission in Multiply Charged Molecular Clusters: Experiment and Theory. *J. Chem. Phys.* **2017**, *146*, 164302.

(43) Last, I.; Levy, Y.; Jortner, J. Fragmentation Channels of Large Multicharged Clusters. *J. Chem. Phys.* **2005**, *123*, 154301.

(44) Wang, W.; Zhao, W.; Hua, L.; Hou, K.; Li, H. Dependence of Multiply Charged Ions on the Polarization State in Nanosecond Laser-Benzene Cluster Interaction. *Chem. Phys. Lett.* **2016**, *652*, 239–242.